Land use and land cover classification with Machine Learning as a subsidy for the estimation of emerging fragility with Geoprocessing: a case study of a watershed in Saquarema, RJ, Brazil

Vitor Ottoni Pastore[1], Vivian Castilho da Costa[2]

[1] Technical School Support Foundation - Ferreira Viana State Technical School - 20271-202 Rio de Janeiro, Brazil
[2] State University of Rio de Janeiro - Department of Physical Geography - 20550-013, Rio de Janeiro, Brazil
pastorevo@gmail.com

Abstract
Considering the importance of land use and land cover for environmental fragility estimation, as it is the primary theme for calculating emerging fragility, this study aimed to evaluate algorithms for classifying open-access optical satellite images with greater spatial resolution than those used by the Mapbiomas Project and others. Statistical and Machine Learning classifiers were tested for a watershed located in a municipality indicated as susceptible to gravitational mass movements and flooding in the state of Rio de Janeiro, Brazil. We used a SPOT-5 satellite image for 2010 and a CBERS-4A WPM for 2020, which were processed and classified in terms of land use and land cover using algorithms plugins added to the open-source GIS QGIS. The algorithms tested were Maximum Likelihood Classification, Minimum Distance, Spectral Angle Mapper, Gaussian Mixture Model, Random Forest, Support Vector Machines, K-Nearest Neighbors, LIBSVM and Object-based Image Analysis. The accuracy assessment and the visualization of Google Earth Pro historical images allowed to select the best results obtained with the two images, which were edited to increase the quality of the classifications. For both images, the best results used Machine Learning algorithms (LIBSVM for t1 and Gaussian Mixture Model for t2), which showed improvements in accuracy after post-classification editing (0.73 to 0.85, and 0.67 to 0.68, respectively). The importance LULC estimate with high resolution Remote Sensing data and powerful algorithms were highlighted for calculating emergent fragility mainly for watersheds, micro-watersheds and small areas, so that it can support research and actions aimed at reducing environmental fragility.

Keywords
Land Cover, Algorithms, Environmental Fragility, Geographic Information System, Digital Image Processing.

1. Introduction

The environmental disasters that have occurred in Brazil, especially during the first two decades of the 21st century, have highlighted the urgent need for effective proposals to reduce environmental fragility, susceptibilities and risks. The mega-disaster in and around Rio de Janeiro's Mountain Region in 2011 was the environmental disaster of the greatest proportions and damage ever recorded in Brazil by the National Center for Risk and Disaster Management (Brazil, 2012). That event triggered a new National Civil Protection and Defense Policy, the creation of the National Center for Monitoring and Prevention of Natural Disasters (National Center for Monitoring and Early Warning of Natural Disasters, n.d.) and the National Plan for the Prevention and Control of Natural Disasters which was launched by the Federal Government in 2012 (Mendonça & Buffon, 2021).

Floods in the state of Rio Grande do Sul led to flooding in several municipalities between the end of April and the beginning of May of 2024. Despite the floods that occurred in the previous year (Guimarães, 2024) and floodgate systems to contain that around the largest cities, there was no adequate maintenance and no planning to mitigate these risks (Federal Council of Engineering and Agronomy, 2024), and an SOS Rio Grande do Sul portal was launched with

information and services from the state government in response to the effects of these floods (Government of the State of Rio Grande do Sul, 2024).

Most environmental studies are carried out for regions with high human population density and large urban areas, while there is less technical-scientific interest in other regions. Despite this, the environmental and socio-economic problems occurring in metropolitan regions have stimulated the migration of groups with lower economic status to adjacent regions and susceptible areas to disasters, increasing the pressure on biodiversity, bodies of water, soils and the topographical features of hillside areas. These changes to the natural environment cause environmental impacts, especially where there is inefficient territorial planning and the presence of ecosystems that should be protected, according to Brazilian environmental legislation.

According to Porto and Porto (2008), "the ideal size of a watershed is one that incorporates all the issues of interest" (p. 45), and the micro-watershed is the most suitable for defining priorities, user participation, pinpointing diffuse problems and operationalizing resources, and is indicated as the basic unit for the sustainable planning and management of rural activities (Souza & Fernandes, 2000). Furthermore, the association between morphometric characteristics, geoprocessing techniques and tools for Territorial Environmental Management tends to increase the efficiency of land use planning when carried out for micro-watersheds (Brum et al., 2020).

The choice of a relevant watershed for landslides and floods in the municipality of Saquarema led to the Mato Grosso River Watershed, which lacks published studies in this area and planning for its management (Figueira, 2009), as well as a history of these events and occurrences reported in 2022. It is also a commuting point between the municipalities of Saquarema and Marica, located in the Metropolitan Mesoregion of Rio de Janeiro (MMRJ), via the RJ-106 highway, where landslides are frequent in the steepest areas and erosive features are located on slopes, and the RJ-118 highway, which has a stretch close to floodplains (Geological Survey of Brazil, 2019).

Several research in Geography have analyzed potential, or natural, fragility and emerging, or anthropically influenced, fragility to estimate environmental fragility (Ross, 1994), as input to analyses of susceptibility and risk of landslides and flooding (Silva, 2006).

As for potential fragility, in Brazil there are disponible municipal maps of susceptibility to gravitational mass movements and flooding for the most susceptible municipalities since 2012 on the 1:25,000 and 1:50,000 scales (Geological Survey of Brazil, 2019). In addition, it is possible to estimate fragility and environmental risk with indirect data made available by public institutions, such as the Brazilian Institute of Geography and Statistics (IBGE) and the National Institute for Space Research (INPE) - and by participatory mapping on the OpenStreetMap (OSM) portal.

For emerging fragility, the key factor is the classification of land use and land cover (LULC), which can be estimated with geographic data in Geographic Information System (GIS).

Although the Mapbiomas Project (2024) provides LULC classification images free of charge for the whole of Brazil from 1985 to 2022 (Collection 8 with 30m spatial resolution) and from 2016 to 2022 (Collection Beta with 10m spatial resolution), studies of emerging and environmental fragility for smaller areas, such as neighborhoods and micro-watersheds, require data with a larger scale of application, such as from Remote Sensing images with higher spatial resolution. In this sense, images obtained by optical sensors located in both drones and orbital satellites can be used, and there are free multispectral Digital Image Processing alternatives in open-source GIS. An example of this application is the classification of LULC using images from the WPM sensor on the CBERS satellite (Sino-Brazilian partnership) version 4A in the open-source QGIS software.

Among the most widely used LULC classifiers with medium and high spatial resolution satellite images are the traditional statistics-based algorithms called Maximum Likelihood Classification (MLC), Minimum Distance and Spectral Angle Mapper; and Machine Learning (ML) algorithms, such as Support Vector Machines (SVM), Random Forest (RF), Artificial Neural Networks (ANN), Convolutional Neural Networks (CNN), K-Nearest Neighbors (KNN), among others (Lary et al., 2016; Alshari & Gawali, 2021; Fagundes; Alixandrini Júnior, 2022; Yuh et al., 2023). Statistical and Machine Learning algorithms for classifying LULC can be executed by programming codes in GIS, or from plugins installed in these programs.

Considering the diversity of LULC classifiers and the need for detailed LULC classifications for micro-watershed studies, this study aims to evaluate LULC classification algorithms with free satellite images for the Mato Grosso River Watershed in Saquarema, Rio de Janeiro State, Brazil.

2. Methods

In order to estimate the LULC of the Mato Grosso River Basin in the two study periods (t1 and t2) proposed by Pastore (2023), images with visible spectrum bands were researched for the Mato Grosso River Basin and for the municipality of Saquarema.

The period considered for t1 was from January 2009 to December 2011, while for t2 it was from January 2019 to December 2021, with less cloud cover over the study area and images from the same season selected for t1 and t2.

For the t1 period, images were found from the SPOT-5 satellite, which are available for free download for Brazil, with processing level L1A (radiometric correction), under the SPOT World Heritage Program of the French Space Agency's National Center for Space Studies (Nosavan, Moreau, & Hosford, 2020). Thus, the multispectral images (NIR-R-G-SWIR bands) and the panchromatic band of the SPOT-5 satellite from September 4, 2010 were selected for t1.

For the t2 period, images from the CBERS-4A WPM sensor satellite from June 22, 2020 were used due to their higher spatial resolution compared to the CBERS-4 and Constellation Planet alternatives.

The characteristics of the multispectral images used for t1 and t2 are shown in Table 1.

Table 1. Multispectral images used for t1 and t2.

	t1	t2
Satellite	SPOT-5	CBERS-4A
Sensor	HRG-2	WPM
Processing level	L1A	L4
Date	2010/09/04	2020/06/22
Spatial resolution	PAN (5m); R, G and NIR (10m); SWIR (10m*)	PAN (2m); RGB and NIR (8m)
Spectral resolution	0.48 – 0.71 µm (PAN) 0.50 – 0.59 µm (G) 0.61 – 0.68 µm (R) 0.78 – 0.89 µm (NIR) 1.58 – 1.75 µm (SWIR)	0.45 – 0.90 µm (PAN) 0.45 – 0.52 µm (B) 0.52 – 0.59 µm (G) 0.63 – 0.69 µm (R) 0.77 – 0.89 µm (NIR)
Radiometric resolution	8 bits	10 bits
Temporal resolution	26 days	31 days
Operating period	2002/05/04 to 2015/03/31	2019/12/20 to current

Legend: * SPOT-5 SWIR band generated at 20m and resampled at 10.
Source: French Space Agency's National Center for Space Studies, 2023; National Institute for Space Research, 2023.

The satellite images used for t1 were processed using spectral conversion, false-color composite generation, removal of the mid-infrared band (SWIR), fusion of the near-infrared, red, green (NIR-R-G) false-color composition with the 5m panchromatic band (PAN), georeferencing, reprojection to the project coordinate system (EPSG:31983), clipping with the boundaries of the Mato Grosso River Basin and definition of symbology parameters for better visualization. These procedures were mostly carried out in the open-source GIS QGIS, while spectral conversion and false-color composition tools were executed in the commercial GIS - test version - ArcGIS Pro (Pastore, 2023).

For t2, all the procedures were carried out in QGIS: red, green, blue and near-infrared (R-G-B-NIR) mosaic and fusion of the composition with the PAN band in the CBERS-4A Downloader plugin, reprojection to EPSG:31983 and clipping with the boundaries of the Mato Grosso River Micro basin.

The LULC classification of t1 was carried out in the SCP and dzetsaka QGIS' plugins, considering training samples generated in SCP, with visualization by historical Google Earth Pro images closest to the date of t1 and images of the LULC classifications of the Mapbiomas Project (2023) with a spatial resolution of 30 m for 2010 (Collection 7) and 10 m for 2020 (Collection 8). The classes defined according to Collection 7 (Mapbiomas Project, 2023) were considered, and classes present in the two classifications were considered in the LULC classification, which received the values and colors from Collection 7 of the Mapbiomas Project (2023). The SCP polygon layer of the samples generated in the SCP Dock Panel was exported as a shapefile, which included the name and code of each class.

In order to compare results obtained from the supervised classification of LULC by traditional and Machine Learning algorithms, classifiers available in the SCP, dzetsaka and OTB plugins of QGIS were used, which were indicated in academic studies (Lary et al., 2016; Alshari & Gawali, 2021; Fagundes & Alixandrini Júnior, 2022; Yuh et

al., 2023) and applied by Pastore (2023). The following classifiers were used: MLC, Minimum Distance and Spectral Angle Mapper, available in SCP; Gaussian Mixture Model, RF, SVM and KNN, available in dzetsaka; classifier training (LIBSVM) and Object-based Image Analysis (OBIA), available in Orfeo ToolBox (OTB). The methods and respective authors of each step-by-step procedure were described by Pastore (2023).

The characteristics of the study area, such as landscape heterogeneity, spectral similarity, spatial resolution, noise, topography, and the quality of training data, all influence the choice and performance of different classifiers. While more complex classifiers like RF, SVM, and OBIA tend to be more adaptable to various conditions, simpler classifiers like MLC and Minimum Distance may fail under complex or variable conditions. Understanding these influences is crucial for selecting the appropriate classifier and optimizing its performance in a given study area. Regarding the limitations of the algorithms used, MLC assumes that the data follow a normal distribution, which is not always the case, especially in complex LULC classes, it requires a considerable number of training samples to produce reliable results, and it may have difficulty separating classes with similar spectral characteristics. Minimum Distance uses Euclidean distance for classification, which may be inadequate in cases where classes are not linearly separable, it does not take into account variability within classes, which may lead to inaccurate classifications, and it may not be effective for classes with complex or overlapping spectral patterns. Spectral Angle Mapper relies on spectral angle and can be highly sensitive to noise present in the data, it measures the angle between spectral vectors, ignoring magnitude, which may lead to errors in situations where magnitude is relevant; and it may not distinguish well between classes that have very close spectral angles. Gaussian Mixture Model requires computationally intensive model training, especially for large data sets, works best with data that has been well processed to eliminate noise and outliers, and may converge slowly or not at all in cases of very complex data. RF can be biased towards the majority class if the classes are not balanced, involves multiple decision trees, making the interpretation of how the classification was performed a complex procedure, and requires careful tuning to avoid loss of generalization ability. SVM can be computationally intensive, requires data normalization, and may not work well if the classes are not clearly separable. KNN is computationally intensive for large data sets, as it needs to calculate the distance for all points, is sensitive to noise and the presence of outliers, and requires tuning of the k parameter. SVM and LIBSVM require hyperparameter tuning, have high computational complexity, and may be limited to the use of a specific set of kernels, which restricts flexibility. OBIA, on the other hand, requires complex segmentation; depends heavily on the quality of the segmentation and the definition of the objects; and requires specialized knowledge to correctly define segmentation and classification parameters (Richards & Jia, 2006; Hastie, Tibshirani & Friedman, 2009; Blaschke, 2010; Mountrakis, Im & Ogole, 2011; Lillesand, Kiefer & Chipman, 2015; Belgiu & Dragut, 2016).

The accuracy analysis was carried out by calculating the Kappa coefficient in the SCP plugin and visualizing historical images in Google Earth Pro for all the algorithms, both for t1 and t2. For this purpose, different samples from those used in the classification for each LULC class were used, and the quality assessment of each classification by the Kappa coefficient indicated by Landis and Koch (1977) was considered. According to the authors, the classification quality is classified as terrible when Kappa coefficient it is below 0.00, bad from 0.0 to 0.2, reasonable from 0.2 to 0.4, good from 0.4 to 0.6, very good from 0.6 to 0.8, and excellent from 0.8 to 1.0.

The best LULC classification results from t1 and t2 were converted to vector layers, then edited and the kappa coefficient was calculated again to check whether the result had improved.

3. Results

Despite the highest Kappa coefficient obtained in the classification of the LULC of t1 with the Gaussian Mixture Model algorithm (0.78) - dzetsaka plugin - (Fig. 1), the classification with the least visible errors identified with historical images from Google Earth Pro was that carried out with the LIBSVM algorithm (Kappa 0.73), which showed a value of 0.85 for this coefficient after vector editing of the LULC classification.

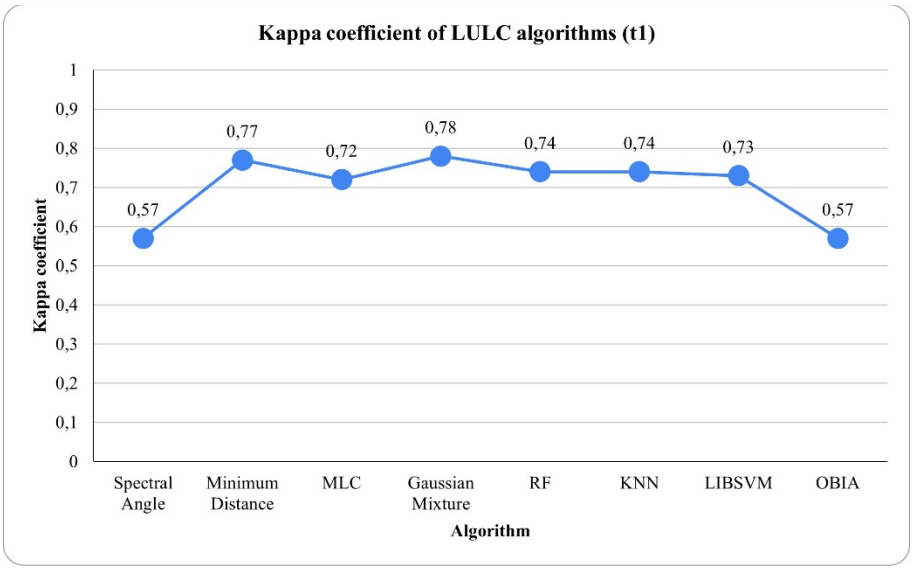

Fig. 1. Classifiers' Kappa indexes for t1 (SPOT-5 HRG-2).

For t2, the Kappa coefficient for the best LULC classification was obtained by applying the Gaussian Mixture Model algorithm - dzetsaka plugin - (Fig. 2), which had a value of 0.67 (very good classification), increasing to 0.68 after vector editing.

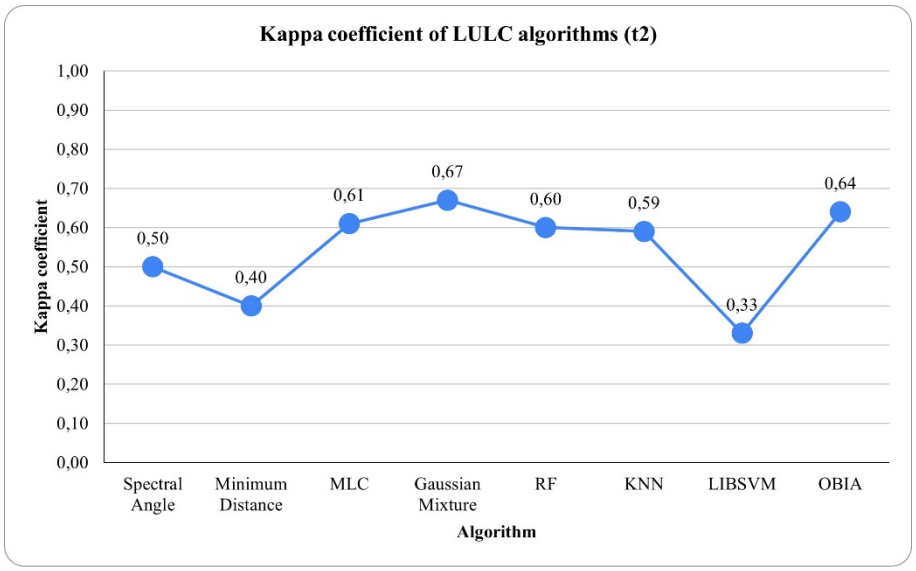

Fig. 2. Classifiers' Kappa indexes for t2 (CBERS-4A WPM).

Thus, for both t1 and t2 the best LULC classification results were obtained from Machine Learning algorithms.

4. Discussion

The best results when applying this methodology to the satellite images used were obtained with Machine Learning algorithms. Although the Kappa coefficient indicated high values for other classifiers, such as Minimum Distance and MLC in t1, these were disregarded after checking with historical images from Google Earth Pro. For t2, the results with statistical algorithms were disregarded because only one classifier showed very good quality (MLC with Kappa 0.61), with several classification errors identified with historical images.

Pastore (2023) found that LULC, the only subject of emerging fragility, was the most influenced factor of the environmental fragility calculation for both t1 and t2. In this sense, the importance of a more detailed estimate of LULC for calculating emergent and environmental fragility is reinforced, to subsidize studies, plans and actions to reduce environmental fragility in micro-watersheds and to develop predictive scenarios of environmental fragility.

It should be noted that in the emerging fragility of t1 and t2 calculations carried out by Pastore (2023), the LULC classes were reclassified according to the fragility levels of each LULC class proposed by Crepani et al. (2001), Ross (1994) and Silva (2006). Emergent fragility and potential fragility (physical factors of the environment) were used to calculate environmental fragility, after which a predictive scenario of environmental fragility for 2030 was estimated using the Land Change Modeler module of the commercial GIS IDRISI Selva 17.0.

5. Conclusions

Machine Learning algorithms showed better results than statistical classifiers, reinforcing the potential of these techniques in classifying LULC.

About satellites with high and very high-resolution images, they can be obtained by assignment or by acquisition at differentiated prices by the Public Administration through consultations. These images can enhance the analysis of damage prevention due to extreme weather events and the promotion of mitigating solutions. Also, greater environmental fragility areas and exposure of people and property to landslides or flooding, monitoring and drone imaging, especially in flatter areas, appear to be more detailed methods for obtaining the images needed to study environmental fragility and propose mitigating solutions. In addition, the use of images from Google Earth Pro software, although available for t1 and t2, are only suitable for viewing on screen, with the potential for visual interpretation for different instants of t1 and t2, as well as to support the generation of LULC samples and assess the classifications accuracy, but are not applicable to the Digital Image Processing.

The acquisition of radar products, such as from ICEYE images (50cm spatial resolution), is a solution for monitoring environmental disasters that can be taken up by municipalities and river basin committees. The characteristics of these products make it possible to assess conditions before and after extreme events, as well as to define with greater precision and in relation to time series, the area's most susceptible to mass movements and flooding, as well as the most fragile areas and the priority areas for mitigation, in the period assessed or estimated for future conditions. This could be a solution for monitoring the application of potential mitigation practices. Furthermore, this technology could be simplified in later decades, such as by automated applications in QGIS plugins, as well as in other integrations between this GIS and the SNAP Digital Image Processing software.

Analysis and scenarios with more recent t1 periods will be able to rely on images with greater spatial, spectral, radiometric and temporal resolution, obtaining more detailed information for planning this and other watersheds. Incorporating additional time points into environmental analyses can greatly enhance the accuracy and reliability of conclusions and predictions. By capturing long-term trends, cyclical patterns, and anomalies, and by refining predictive models, the analysis becomes more robust. This leads to a more nuanced understanding of future environmental fragility, better informs policy and management decisions, and ultimately contributes to more effective environmental conservation and risk mitigation strategies (Verbesselt et al., 2010). This includes multispectral images from the Planet satellite constellation and Sentinel-2 satellite versions, as well as the acquisition of commercial multispectral, hyperspectral and more detailed topographic images. Integrating hyperspectral and radar imagery into LULC classifications enhances accuracy by providing richer spectral and structural information, improving the quality of training data, which allows for better differentiation between classes, particularly in complex or heterogeneous landscapes, and provides a more comprehensive understanding of environmental processes.(Galvão, Formaggio & Tisot, 2009; Gomez-Chova et al., 2015). Consequently, the LULC classifications become more reliable, leading to more accurate predictions.

The LULC mapping updates from the Mapbiomas, Dynamic World and Esri Land Cover projects, as well as from federal, state and municipal institutions, will be able to form the LULC layers of t1 and t2 and it will be possible to assess the need for image classification, but we recommend comparing the results with estimates using robust algorithms, such as Machine Learning classifiers. In addition, the vectorization of samples or the total areas of each class in the field, by specialists with equipment of greater positional accuracy, can surpass the quality of the other methods, when this method is a viable option depending on the size and complexity of the study area.

References

Alshari, E. A., & Gawali, B. W. (2021). Development of classification system for LULC using remote sensing and GIS. *Global Transitions Proceedings*, 2(1), 8-17. **https://dx.doi.org/10.1016/j.gltp.2021.01.002**

Belgiu, M., & Dragut, L. (2016). Random forest in remote sensing: A review of applications and future directions. *ISPRS Journal of Photogrammetry and Remote Sensing*, 114, 24-31. **https://doi.org/10.1016/j.isprsjprs.2016.01.011**

Blaschke, T. (2010). Object based image analysis for remote sensing. *ISPRS Journal of Photogrammetry and Remote Sensing*, 65 (1), 2-16. **https://doi.org/10.1016/j.isprsjprs.2009.06.004**

Brazil. (2012). *Brazilian Yearbook of Natural Disasters - 2012*. National Secretariat for Regional and Urban Development. National Secretary for Protection and Civil Defense of Brazil. National Center for Risk and Disaster Management.
https://www.icict.fiocruz.br/sites/www.icict.fiocruz.br/files/AnuariodeDesastresNaturais_2012.pdf

Brum, M. L., Bernardi, E. C. S., Moreti, G. B., Panziera, A. G., & Swarowsky, A. (2020). Flood relations with morphological characterization of the hydrographic micro watershed of Lajeado do Moinho in the City of São Sepé - RS. *Anuário do Instituto de Geociências - UFRJ*, 3 (43), 436-443. **https://dx.doi.org/10.11137/2020_3_436_443**

Crepani, E., Medeiros, J. S., Hernandez Filho, P., Florenzano, T. G., Duarte, V., & Barbosa, C. C. F. (2001). Remote Sensing and Geoprocessing applied to the ecological and economical zoning and to the territorial ordering. National Institute for Space Research. National Secretary of Science, Technology and Innovation of Brazil. **http://www.dsr.inpe.br/laf/sap/artigos/CrepaneEtAl.pdf**

Fagundes, W. S., & Alixandrini Júnior, M. J. (2022). Evolution of remote sensing image classification techniques used in Brazilian scientific production. *Revista Geociências*, 41 (3), 593-604. **https://dx.doi.org/10.5016/geociencias.v41i03.16209**

Federal Council of Engineering and Agronomy. (2024). *Para ajudar a compreender a tragédia do Rio Grande do Sul* . **https://www.confea.org.br/index.php/para-ajudar-compreender-tragedia-do-rio-grande-do-sul**

Figueira, R. B. (2009). Caracterização Sócio-Ambiental e Ordenamento Territorial para a Bacia do Rio Mato Grosso – Saquarema – RJ. *Caminhos de Geografia*, 10 (30), 142-152. **https://dx.doi.org/10.14393/RCG103015962**

French Space Agency's National Center for Space Studies. (2023). *SPOT 1 to 5 satellites*. **http://spot5.cnes.fr/gb/systeme/3110.htm**

Galvão, L. S., Formaggio, A. R., & Tisot, D. A. (2009). Discriminação de variedades de cana-de-açúcar com dados hiperespectrais do sensor Hyperion/EO-1. *Revista Brasileira de Cartografia*, 57 (1). **https://doi.org/10.14393/rbcv57n1-44957**

Government of the State of Rio Grande do Sul. (2024). SOS Rio Grande do Sul. State Secretary of Communication. h **ttps://sosenchentes.rs.gov.br/inicial**

Guimarães, M. B. (2011). Mudança e colapso no Litoral Fluminense: os sambaquieiros e os outros no Complexo Lagunar de Saquarema, RJ. *Revista do Museu de Arqueologia e Etnologia*, 21, 71-91. **https://dx.doi.org/10.11606/issn.2448-1750.revmae.2011.89962**

Geological Survey of Brazil. (2019). *Carta de suscetibilidade a movimentos gravitacionais de massa e inundação*: município de Saquarema, RJ. **http://rigeo.cprm.gov.br/jspui/handle/doc/21438**

Gomez-Chova, L. et al. (2015). Multimodal Classification of Remote Sensing Images: A Review and Future Directions. *Proceedings of the IEEE*, 103 (9), 1560-1584. **https://doi.org/10.1109/JPROC.2015.2449668**

Hastie, T., Tibshirani, R., & Friedman, J. (2009). *The Elements of Statistical Learning: Data Mining, Inference, and Prediction* (2nd ed.). Springer.

Landis, J. R., & Koch, G. G. (1977). The measurement of observer agreement for categorical data. *Biometrics*, 33(1), 159-174. **https://dx.doi.org/10.2307/2529310**

Lary, D. J., Alavi, A. H., Gandomi, A. H., & Walker, A. L. (2016). Machine learning in geosciences and remote sensing. *Geoscience Frontiers*, 7(1), 3-10. **https://doi.org/10.1016/j.gsf.2015.07.003**

Lillesand, T. M., Kiefer, R. W., & Chipman, J. W. (2015). *Remote Sensing and Image Interpretation* (7th ed.). John Wiley & Sons.

Mapbiomas Project. (2024). *Downloads*. **https://brasil.mapbiomas.org/en/downloads**

Mendonça, F., & Buffon, E. A. M. (2021). Riscos híbridos. In: Mendonça. F. (Org.). *Riscos híbridos: concepções e perspectivas ambientais*. São Paulo: Oficina de Textos, 1. ed., 13-38.

Mountrakis, G., Im, J., & Ogole, C. (2011). Support vector machines in remote sensing: A review. *ISPRS Journal of Photogrammetry and Remote Sensing*, 66 (3), 247-259. **https://doi.org/10.1016/j.isprsjprs.2010.11.001**

National Center for Monitoring and Early Warning of Natural Disasters. (n.d.) History of CEMADEN's creation. **http://www2.cemaden.gov.br/historicoda-criacao-do-cemaden**

National Institute for Space Research. (2023). *Divisão de Geração de Imagens*: Catálogo. National Secretary of Science, Technology and Innovation of Brazil. **http://www.dgi.inpe.br/catalogo/explore**

Nosavan, J., Moreau, A., & Hosford, S. (2020). SPOT World Heritage catalogue: 30 years of SPOT 1-to-5 observation. *EGU General Assembly 2020*. **https://dx.doi.org/10.5194/egusphere-egu2020-8275**

Pastore, V. O. (2023). Analysis of environmental fragility scenario and indication of mitigating areas in the Mato Grosso River Watershed, municipality of Saquarema, RJ. [Doctoral dissertation, Universidade do Estado do Rio de Janeiro]. Biblioteca Digital de Teses e Dissertações da Universidade do Estado do Rio de Janeiro. **https://www.bdtd.uerj.br:8443/handle/1/21868**

Porto, M. F. A., & Porto, R. L. (2008). Gestão de bacias hidrográficas. *Estudos Avançados*, 63 (22), 43-60. **http://dx.doi.org/10.1590/s0103-40142008000200004**

Richards, J. A., & Jia, X. (2006). *Remote Sensing Digital Image Analysis: An Introduction*. Springer.

Ross, J. L. S. (1994). Análise empírica da fragilidade dos ambientes naturais e antropizados. *Revista do Departamento de Geografia*, 8, 63-74. **https://dx.doi.org/10.7154/RDG.1994.0008.0006**

Silva, D. A. (2006). *Environmental zoning of a segment of Parque Estadual da Cantareira (Cantareira State Park) and its borders crossed by Fernão Dias Highway (BR 381)* [Doctoral dissertation, Universidade de São Paulo]. USP Digital Library of Academic Works. **https://doi.org/10.11606/T.8.2006.tde-19062007-155319**

Souza, E. R., & Fernandes, M. R. (2000). Sub-bacias hidrográficas: unidades básicas para o planejamento e a gestão sustentáveis das atividades rurais. *Informe Agropecuário*, Belo Horizonte, 21 (207), 15-20. **http://www.cecs.unimontes.br/biblioteca_virtual/detalhardoc.php?id=2125**

Verbesselt, J., Hyndman, R., Newnham, G., & Culvenor, D. (2010). Detecting trend and seasonal changes in satellite image time series. Remote Sensing of Environment, 114 (1), 106-115. **https://doi.org/10.1016/j.rse.2009.08.014**

Yuh, Y. G., Tracz, W., Matthews, H. D., & Turner, S. E. (2023). Application of machine learning approaches for land cover monitoring in northern Cameroon. *Ecological Informatics*, 74, 1-15. **http://dx.doi.org/10.1016/j.ecoinf.2022.101955**